JCTC Journal of Chemical Theory and Computation

Spin-Unrestricted Calculations of Bare-Edged Nanographenes Using DFT and Many-Body Perturbation Theory

Rodolphe Pollet*,† and Hakim Amara‡

DSM/IRAMIS/SPAM-LFP, CEA, Gif-sur-Yvette, France, and Laboratoire d'Etude des Microstructures, ONERA-CNRS, Châtillon, France

Received April 15, 2009

Abstract: The ability of Density Functional Theory to predict the electronic and magnetic properties of semi-infinite graphene with a single bare edge has been probed. In order to improve the accuracy of spin-unrestricted calculations performed with semilocal density functionals, higher-level methods including double hybrid density functionals and many-body perturbation theory have been applied to the polycyclic aromatic hydrocarbons model systems. We show that the antiferromagnetic or ferromagnetic tendencies of the corresponding electronic ground states strongly depend on the choice of the density functional. In addition the relative stability of the armchair and zigzag edges has been investigated, emphasizing the importance of using methods beyond semilocals density functionals.

Graphene, which is a monolayer of carbon atoms packed into a dense honeycomb crystal structure, belongs to the rich world of carbon nanostructures.[1] It has been the subject of intense scrutinity,[2,3] especially because this kind of structure was previously presumed not to exist in the free state. This exciting object, with unusual electronic and magnetic properties, is considered to be among the most important materials for nanoscale device applications.[4] However, all those remarkable properties can be strongly affected by the presence of edges which are in general a combination of armchair and zigzag regions.[5−7] In particular, theoretical and experimental studies have been devoted to the demonstration that edges of graphene substantially modify their electronic and magnetic properties.[8−10] Therefeore, much effort has been focused on the study of the edges in graphitic nanomaterials, such as graphene and also nanotubes. Indeed, the strong adhesion between the edge of a tube and the metal clusters from which they are produced is a requirement for the nanotube growth.[11]

Graphene exists as flakes also called nanographenes or, for the smallest sizes, polycyclic aromatic hydrocarbons (PAHs). A large spectrum of theoretical methods can therefore be applied according to the size of the system, ranging from intuitive (semiempirical) tight-binding models to highly accurate (ab initio) wave function based methods. Electronic structure calculations of nanomaterials extensively rely on Density Functional Theory (DFT) and especially on semilocal approximations to the exchange-correlation density functional, such as the Local Density Approximation (LDA) or Generalized Gradient Approximation (GGA).[12] The favorable computational cost of these methods together with periodic boundary conditions (PBC) have allowed calculations on infinite or semi-infinite graphene,[13−17] using the pseudopotential plane-waves method. In addition single-hybrid approximations, incorporating a small proportion of exact exchange, have been used for periodic graphenes thanks to a screening procedure.[18−20] Finite nanographenes have also been studied using DFT with a strong focus on hydrogen-terminated PAHs[20−22] (save one exception[23]).

In this Letter, we adopt a new approach, using many-body perturbation theory as well as more elaborate density functionals, to investigate the electronic and magnetic properties of edges present in PAHs. Different PAHs are considered with all the edges hydrogenated but one, thus mimicking semi-infinite graphenes with bare active sites. One can expect that such higher-level methods should indeed be required for an accurate description of edges. This is necessary to understand the key role played by edges in the modification of the properties of PAH as well as their reactivity.

The efficiency of semilocal approximations has been probed by using the Perdew-Burke-Ernzerhof (PBE)[24] GGA density functional in conjunction with triple-ζ plus polarization Gaussian basis sets (TZVPP) and the resolution-of-the-identity (RI) approximation[25] implemented in the TURBOMOLE quantum chemical program package version 5.10.[26] Approximations depending not only on the electron density and on its gradient but also on the Kohn−Sham orbital kinetic energy density, called Meta-Generalized Gradient Approximations (Meta-GGA), have also been considered with the TPSS[27] nonempirical density functional. Wave function based methods constitute a usually more accurate but also time-consuming alternative. For medium-sized systems, second order Møller−Plesset (MP2) perturbation

* Corresponding author e-mail: rodolphe.pollet@cea.fr.
† CEA Saclay.
‡ Onera Châtillon.

10.1021/ct900184d CCC: $40.75
Published on Web 06/01/2009

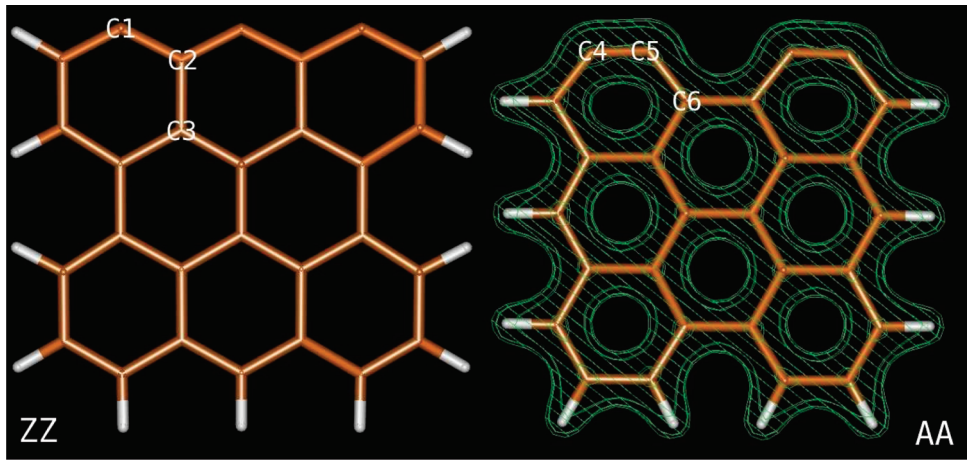

Figure 1. Zigzag (ZZ) and armchair (AA) edges of the bare-edged PAH[3,3] system optimized at the PBE/TZVPP level of theory. For AA, contours of the PBE electronic density are also plotted.

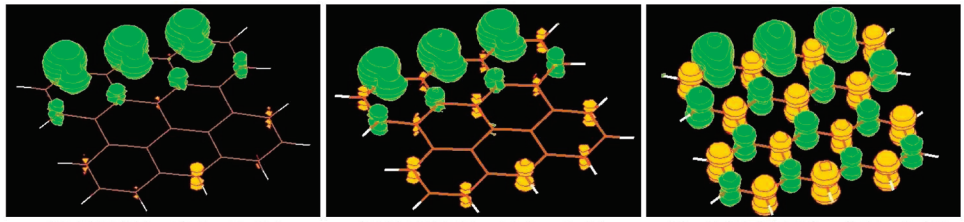

Figure 2. Spin density (green positive, yellow negative) for the zigzag edge of PAH[3,3] obtained with the PBE, TPSS, and B2-PLYP density functionals. The expectation value of the $\mathbf{S^2}$ operator is also reported.

theory (together with the RI approximation) represents an affordable yet powerful method in comparison with DFT, especially in the case of dispersive interactions. Recently a simple, partly empirical, improvement of the method has been proposed by scaling the spin components (SCS) of the pair correlation energies.[28] Like its parent method, the SCS-MP2 method can however fail to describe open-shells species, such as the zigzag (bare) edge of PAHs (*vide infra*). Double-hybrid density functionals (DHDF),[29,30] which lie between pure density and wave function approaches, appear more robust with regard to spin contamination problems occurring in spin-unrestricted calculations.[31] The double hybrid functional tested in this work (B2-PLYP) mixes the B88[32] exchange functional with Hartree−Fock-like exchange and LYP[33] correlation functional with MP2-like correlation energy.

Due to the presence of unpaired electrons along the zigzag (ZZ) edge of graphene, special care must be taken to ensure that first principles calculations correctly reproduce the spin density distribution, i.e., $\rho_s(\mathbf{r}) = \rho_\alpha(\mathbf{r}) - \rho_\beta(\mathbf{r})$, of the electronic ground state.[23] Prior to the energetical comparison between both edges, methods causing a deterioration of $\rho_s(\mathbf{r})$ must therefore be identified and better avoided. This investigation has begun with the bare-edged PAH[3,3] system (28 carbon and 11 hydrogen atoms), where [*x*,*y*] specify the number of adjacent cycles in the horizontal (*x*) and vertical (*y*) directions (see Figure 1). Isosurfaces corresponding to the PBE, TPSS, and B2-PLYP density functionals are reported in Figure 2 together with the expectation value of $\mathbf{S^2}$. Whether the latter value should be used as a diagnostic tool to judge the quality of a spin-unrestricted calculation is still controversial as far as DFT is concerned because only the noninteracting Kohn−Sham wave function is used for the estimation.[34] In this case a clear correlation between the error on $\langle \mathbf{S^2} \rangle$ (equal to 3.75 for a pure quadruplet) and the delocalization of $\rho_s(\mathbf{r})$ can be observed. This effect is particularly significant in the case of the B2-PLYP functional and can be most probably attributed to the large fraction (≈50%) of exact exchange. For comparison, a spin-unrestricted Hartree−Fock (UHF) calculation results in $\langle \mathbf{S^2} \rangle$ as high as 6.32. All density functionals predict a spin density distribution with large positive contributions corresponding to the unpaired electrons of the unsaturated carbons and smaller negative contributions on the opposite hydrogenated edge due to spin polarization effects. These very characteristics have been also observed for the smaller PAH[4,1] system from B3LYP spin-unrestricted calculations.[23] This is also similar to the antiferromagnetic ground state of PAHs fully saturated by hydrogen.[20,22] We have then considered the larger zigzag bare-edged PAH[5,5] (66 carbon and 17 hydrogen atoms). Again the spin density exhibits a larger delocalization when the double hybrid density functional is used (see Figure 3). Interestingly the largest $\langle \mathbf{S^2} \rangle$ value has been obtained for the PBE calculation, whose convergence was particularly difficult to achieve. But the main difference with respect to the smaller PAH[3,3] system is the spin polarization on the opposite, hydrogenated, edge. Contributions to the spin density on this side are indeed positive for all density functionals, showing a tendency toward ferromagnetism. This is not only in contrast to the case of the PAH[3,3] system but also of the fully hydrogenated PAHs, where the energy of the ferromagnetic state always lies higher than for the antiferromagnetic state.[20,22]

We now compare the structures and energetical stability of the ZZ and AA edges. Geometry optimizations have been

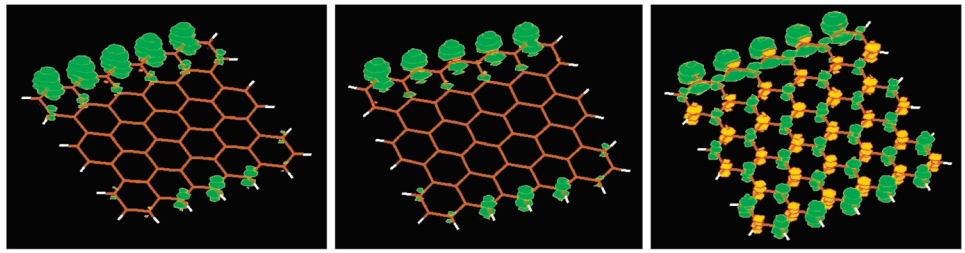

Figure 3. Spin density (green positive, yellow negative) for the zigzag edge of PAH[5,5] obtained with the PBE, TPSS, and B2-PLYP density functionals. The expectation value of the $\mathbf{S}^2$ operator is also reported.

Table 1. Structural Parameters of the Zigzag (ZZ) and Armchair (AA) Edges Obtained from PBE/TZVPP Geometry Optimizations of the PAH[3,3] System (See Labels on Figure *1*)

parameters	PAH[3,3]	∞ nanoribbons
C1−C2 (Å)	1.38	1.37,[35] 1.38,[13] 1.39[15]
C2−C3 (Å)	1.47	1.47[15]
C4−C5 (Å)	1.26	1.23,[13,16,35] 1.24[15]
C5−C6 (Å)	1.38	1.39[15,16]
C4−C5−C6 (°)	127	126[15]

performed at the PBE/TZVPP level of theory. Interestingly the characteristic distances and angle (see Table 1) are in excellent agreement with DFT calculations of infinite nanoribbons. As previously noted,[13,35] the shortening of the C−C bond at the AA edge can be rationalized by the formation of a triple-bond, in agreement with the accumulation of electronic density between both carbon atoms (see Figure 1). The bond length is actually closer to the distance observed in benzyne (1.27 Å)[36] than in acetylene (1.20 Å). The harmonic vibrational frequencies associated with the symmetric and antisymmetric C−C stretch combinations are found at 1921 and 1948 cm^{-1}, respectively. These values are strongly blue-shifted (approximately 400 cm^{-1}) with respect to the other C−C stretches in the 1600−1500 cm^{-1} range: as an example the frequency of the middle C−C bond of the bare edge is found at 1539 cm^{-1}. The present calculations show that evidence for the formation of triple bonds at the armchair edge can be found in the IR spectra of these species. In spite of the weak intensities calculated for these bands, their isolated position in the spectrum should make their experimental observation relatively easy.

Measuring the relative reactivity of both edges should help to identify the best candidate as a precursor to a nanotube growing on a metallic particle. We have calculated the C−H bonds dissociation energy

$$E_{diss} = \frac{1}{n}(E_{bare} + nE_H - E_{H-term}) \qquad (1)$$

where n is the number of unsaturated carbon atoms, E_{bare} is the energy of the bare-edged AA or ZZ system, E_H is the energy of the hydrogen atom, and E_{H-term} is the energy of the fully hydrogenated PAH. Our work has been however not restricted to density functional methods and includes the perturbational approaches detailed previously.[37] Results reported in Table 2 confirm that, except for the MP2 calculation, all methods tested in this work predict that the bare-edged AA structure is more stable than the ZZ one. The SCS procedure succeeds in correcting the MP2 failure and leads to energies in excellent agreement with the double hybrid density functional calculation. Both methods also predict AA and ZZ energies close to the values obtained from DFT calculations of infinite nanoribbons (respectively, 4.36 and 5.36 eV[15]). The PBE density functional significantly underestimates (0.25 eV) the difference between the ZZ and AA dissociation energies, mainly because of too weak C−H bonds at the ZZ edge. We note that the PBE/TZVPP dissociation energy of the ZZ edge is in excellent agreement with the value obtained by May et al.[21] (5.04 eV) on the same system with another GGA density functional. Following Koskinen et al.,[15] the reactivity of both bare-edged structures can also be judged by considering the following reaction

$$\mathrm{P\cdot} + \mathrm{H_2} \xrightarrow{-E'_{diss}} \mathrm{PH} + \mathrm{H\cdot}$$

where P· represents the bare-edged system, PH represents the H-terminated PAH, and E'_{diss} is calculated by subtracting the H_2 dissociation energy to the C−H bonds dissociation energy. The previous reaction can be seen as the first bimolecular reaction step in the mechanism of hydrogenation. According to the values of E'_{diss} reported in Table 3, the bimolecular reaction is endergonic for the AA edge and exergonic for the ZZ edge. The difference is obviously related to the presence of highly reactive dangling bonds in the ZZ case.

In conclusion, magnetic properties resulting from spin-unrestricted DFT calculations are not only influenced by the

Table 2. C−H Bonds Dissociation Energy (eV) for Armchair (AA) and Zigzag (ZZ) Edges of PAH[3,3] Optimized at the PBE/TZVPP Level of Theory[a]

method	AA	ZZ	Δ*E*
PBE/TZVPP	4.37	5.02	0.65
B2-PLYP/TZVPP	4.46	5.36	0.90
MP2/TZVPP	4.34	4.08	−0.27
SCS-MP2/TZVPP	4.44	5.34	0.90

[a] Difference between both values is reported in the last column.

Table 3. Difference between C−H bonds Dissociation Energy and H_2 Dissociation Energy (eV) for Armchair (AA) and Zigzag (ZZ) Edges of PAH[3,3] Optimized at the PBE/TZVPP Level of Theory

method	AA	ZZ
PBE/TZVPP	−0.17	0.48
B2-PLYP/TZVPP	−0.17	0.73
MP2/TZVPP	−0.15	−0.41
SCS-MP2/TZVPP	−0.22	0.68

choice of the density functional, through the delocalization of the spin density, but also by the size of the system, which can alter the relative weight of the antiferromagnetic-like and ferromagnetic-like states. In addition, although all methods tested in this work confirm the stronger stability of the armchair with respect to the zigzag bare edge, semilocal density functionals appear to underestimate this energetical preference. Periodic boundary calculations of nanoribbons using such a method should therefore consider this bias demonstrated here from high level calculations of closely related finite-size systems.

Acknowledgment. The authors thank Eric Gloaguen, Michel Mons, and Cyrille Barreteau (all from CEA/DSM/IRAMIS) for fruitful discussions.

References

(1) Delgado, J. L.; Herranz, M. Á.; Martín, N. *J. Mater. Chem.* **2008**, *18*, 1417.

(2) Novoselov, K. S.; Geim, A. K.; Morozov, S. V.; Jiang, D.; Zhang, Y.; Dubonos, S. V.; Grigorieva, I. V.; Firsov, A. A. *Science* **2004**, *306*, 666.

(3) Zhang, Y.; Tan, Y.-M.; Stormer, H. L.; Kim, P. *Nature* **2005**, *438*, 201.

(4) Castro Net, A. H.; Guinea, F.; Peres, M. R.; Novoselov, K. S. *Rev. Mod. Phys.* **2009**, *81*, 109.

(5) Liu, Z.; Suenaga, K.; Harris, P. J. F.; Ijima, S. *Phys. Rev. Lett.* **2009**, *102*, 015501.

(6) Jia, X.; Hofmann, M.; Meunier, V.; Sumpter, B. G.; Campos-Delgado, J.; Romo-Herrera, J. M.; Son, H.; Hsieh, Y.-P.; Reina, A.; Kong, J.; Terrones, M.; Dresselhaus, M. S. *Science* **2009**, *323*, 1701.

(7) Girit, Ç. Ö.; Meyer, J. C.; Erni, R.; Rossell, M. D.; Kisielowski, C.; Yang, L.; Park, C.-H.; Crommie, M. F.; Cohen, M. L.; Louie, S. G.; Zettl, A. *Science* **2009**, *323*, 1705.

(8) Nakada, K.; Fujita, M.; Dresselhaus, G.; Dresselhaus, M. S. *Phys. Rev. B* **1996**, *54*, 17954.

(9) Son, Y. M.; Cohen, M. L.; Louie, S. G. *Nature* **2006**, *444*, 334.

(10) Enoki, T.; Kobayashi, Y.; Fukui, K. *Int. Rev. Phys. Chem.* **2007**, *26*, 609.

(11) Ding, F.; Larsson, P.; Larsson, J. A.; Ahuja, R.; Duan, H.; Rosén, A.; Bolton, K. *Nano Lett.* **2008**, *8*, 463.

(12) Felice, R. D.; Calzolari, A.; Varsano, D.; Rubio, A. In *Introducing Molecular Electronics*; Cuniberti, G.; Fargas, G.; Richter, K., Eds.; Springer-Verlag: Berlin, 2005; p 77.

(13) Kawai, T.; Miyamoto, Y.; Sugino, O.; Koga, Y. *Phys. Rev. B* **2000**, *62*, R16349.

(14) Gianozzi, P.; Car, R.; Scoles, G. *J. Chem. Phys.* **2003**, *118*, 1003.

(15) Koskinen, P.; Malola, S.; Häkkinen, H. *Phys. Rev. Lett.* **2008**, *101*, 115502.

(16) Okada, S. *Phys. Rev. B* **2008**, *77*, 041408.

(17) Wassmann, T.; Seitsonen, A. P.; Saitta, A. M.; Lazzeri, M.; Mauri, F. *Phys. Rev. Lett.* **2008**, *101*, 096402.

(18) Barone, V.; Hod, O.; Scuseria, G. E. *Nano Lett.* **2006**, *6*, 2748.

(19) Hod, O.; Barone, V.; Peralta, J. E.; Scuseria, G. E. *Nano Lett.* **2007**, *7*, 2295.

(20) Hod, O.; Barone, V.; Scuseria, G. E. *Phys. Rev. B* **2008**, *77*, 035411.

(21) May, K.; Dapprich, S.; Furche, F.; Unterreiner, B. V.; Ahlrichs, R. *Phys. Chem. Chem. Phys.* **2000**, *2*, 5084.

(22) Jiang, D.; Sumpter, B. G.; Dai, S. *J. Chem. Phys.* **127**, *127*, 124703.

(23) Montoya, A.; Truong, T. N.; Sarofim, A. F. *J. Phys. Chem. A* **2000**, *104*, 6108.

(24) Perdew, J. P.; Burke, K.; Ernzerhof, M. *Phys. Rev. Lett.* **1996**, *77*, 3865.

(25) Weigend, F.; Häser, M.; Patzelt, H.; Ahlrichs, R. *Chem. Phys. Lett.* **1998**, *294*, 143.

(26) Ahlrichs, R.; Bär, M.; Häser, M.; Horn, H.; Kölmel, C. *Chem. Phys. Lett.* **1989**, *162*, 165.

(27) Tao, J.; Perdew, J. P.; Staroverov, V. N.; Scuseria, G. E. *Phys. Rev. Lett.* **2003**, *91*, 146401.

(28) Grimme, S. *J. Chem. Phys.* **2003**, *118*, 9095.

(29) Grimme, S. *J. Chem. Phys.* **2006**, *124*, 034108.

(30) Schwabe, T.; Grimme, S. *Acc. Chem. Res.* **2008**, *41*, 569.

(31) Menon, A. S.; Radom, L. *J. Phys. Chem. A* **2008**, *112*, 13225.

(32) Becke, A. D. *Phys. Rev. A* **1988**, *38*, 3098.

(33) Lee, C.; Yang, W.; Parr, R. G. *Phys. Rev. B* **1988**, *37*, 785.

(34) Pople, J. A.; Gill, P. M. W.; Handy, N. C. *Int. J. Quantum Chem.* **1995**, *56*, 303.

(35) Lee, Y. H.; Kim, S. G.; Tománek, D. *Phys. Rev. Lett.* **1997**, *78*, 2393.

(36) Kraka, E.; Cremer, D. *Chem. Phys. Lett.* **1993**, *216*, 333.

(37) In view of the dramatic UHF error on $\langle \mathbf{S}^2 \rangle$, MP2 calculations of the ZZ edge have been performed from restricted open-shell calculations.

CT900184D